

## Adaptive Grid Refinement for Computation of the Homogenized Elasticity Tensor

Ronald H. W. Hoppe, Svetozara I. Petrova, Yuri V. Vassilevski

### Angaben zur Veröffentlichung / Publication details:

Hoppe, Ronald H. W., Svetozara I. Petrova, and Yuri V. Vassilevski. 2004. "Adaptive Grid Refinement for Computation of the Homogenized Elasticity Tensor." *Lecture Notes in Computer Science* 2907: 371–78. [https://doi.org/10.1007/978-3-540-24588-9\\_42](https://doi.org/10.1007/978-3-540-24588-9_42).

### Nutzungsbedingungen / Terms of use:

licgercopyright

Dieses Dokument wird unter folgenden Bedingungen zur Verfügung gestellt: / This document is made available under these conditions:

**Deutsches Urheberrecht**

Weitere Informationen finden Sie unter: / For more information see:

<https://www.uni-augsburg.de/de/organisation/bibliothek/publizieren-zitieren-archivieren/publiz/>



# Adaptive Grid Refinement for Computation of the Homogenized Elasticity Tensor

Ronald H.W. Hoppe<sup>1</sup>, Svetozara I. Petrova<sup>2</sup>, and Yuri V. Vassilevski<sup>3</sup>

<sup>1</sup> Institute of Mathematics, University of Augsburg  
University Str.14, D-86159 Augsburg, Germany

<sup>2</sup> Central Laboratory for Parallel Processing, Bulgarian Academy of Sciences,  
Acad. G. Bontchev, Block 25A, 1113 Sofia, Bulgaria

<sup>3</sup> Institute of Numerical Mathematics, Russian Academy of Sciences,  
8 Gubkina Str., 117333 Moscow, Russia

**Abstract.** Optimal structural design of microstructured materials is one of the central issues of material science. The paper deals with the shape optimization of microcellular biomorphic silicon carbide ceramics produced from natural wood by biotemplating. Our purpose is to achieve an optimal performance of the new composite materials by solving a non-linear optimization problem under a set of equality and inequality constraints. The microscopic geometric quantities serve as design parameters within the optimization procedure. Adaptive grid-refinement technique based on reliable and efficient a posteriori error estimators is applied in the microstructure to compute the homogenized elasticity coefficients. Some numerical results are included and discussed.

## 1 Introduction

Biological materials exhibit a hierarchically designed composite morphology and unique mechanical properties. Natural grown materials like wood and cellulose fibres have recently become of interest for advanced processing of engineering materials. Carbon preforms derived from natural wood structures serve as templates for preparation of microstructural designed materials. The tracheidal cells in wood form directly porous structures at the microlevel which are accessible for liquid or gaseous infiltration and chemical reaction processing. Biomorphic microcellular silicon carbide (SiC) ceramics have been recently produced by biotemplating methods (see [6]). The production process requires infiltration of liquid or gaseous silicon (Si) into the carbonized (at high temperature) wood templates. Due to their excellent structural-mechanical properties, the new ceramic composite materials have found a lot of technical applications, for instance, filter and catalyst carriers, heat insulation structures, medical implants, sensor tools, etc.

In this study, we are concerned with the optimal shape design of the new microstructured ceramics by using the homogenization modelling and mesh-adaptivity at the microlevel. The homogenization design method is well established in structural mechanics (cf., e.g., [2, 4, 5, 7, 8]) and recently successfully applied to a variety of optimization problems. Section 2 comments on the computation of the homogenized elasticity tensor in the case of a stationary microstructure with homogeneous linear elastic constituents. We assume a periodical distribution of the microstructure with a geometrically simple tracheidal periodicity cell. Here, the optimal shape design of the biomorphic SiC ceramics is briefly discussed. The optimization is applied to the homogenized model under both equality and inequality constraints on the state variables and design parameters. In Section 3, we focus on the adaptive refinement method based on the *Zienkiewicz-Zhu* (see [11]) error estimator. Mesh-adaptive procedures and a posteriori error analysis have been recently widely used in many finite element simulations of computational engineering and scientific computing (cf., e.g., [1, 3, 9–11]). Numerical experiments given in the last section show the efficiency of our adaptive strategy and the reliability of the a posteriori error indicator.

## 2 Optimal Shape Design Based on Homogenization

We assume periodical distribution of the microstructure with a simple unit tracheidal periodicity cell  $Y$  (see Fig. 1) consisting of an outer layer of carbon, interior layer of SiC, a very thin layer of silicon dioxide ( $\text{SiO}_2$ ), and a void. Experimental data show that the SiC-ceramics are not stable under oxidizing conditions and they form a  $\text{SiO}_2$ -layer of thickness 100 nm whereas the typical size of the tracheidal cell is approximately 30–50  $\mu\text{m}$  in diameter. The  $\text{SiO}_2$ -coating of the interface between the SiC and the void can be done by a controlled oxidation process of the inner SiC-surfaces at 800–1200 $^\circ\text{C}$  in ambient atmosphere and can significantly improve the mechanical performance of the ceramic materials.

To provide a macroscopic scale model of the biomorphic composites we have applied the homogenization approach which has recently become a well-established technique in structural mechanics to find an optimal design of microstructured materials (cf., e.g., [2, 4, 5, 8, 7]). We consider the case of a stationary microstructure with homogeneous isotropic linear elastic constituents and Hooke's

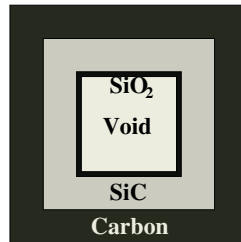


**Fig. 1.** The periodicity cell  $Y$  with 3 constituents and a void

law as the constitutive equation. Under the assumption for well separated macro- and micro-scales, the homogenization method based on double scale asymptotic expansion (we refer to [2, 5, 8] for details) results in the homogenized elasticity tensor  $\mathbf{E}^H = (E_{ijkl}^H)$ ,  $i, j, k, l = 1, 2$ , with

$$E_{ijkl}^H = \frac{1}{|Y|} \int_Y \left( E_{ijkl}(y) - E_{ijpq}(y) \frac{\partial \xi_p^{kl}}{\partial y_q} \right) dy. \quad (1)$$

The vector function  $\xi^{kl}$  with periodic components  $\xi_p^{kl} \in H_{\text{per}}^1(Y)$ ,  $p = 1, 2$ , is considered as a microscopic displacement field of the following elasticity cell-problem in a weak formulation

$$\int_Y \left( E_{ijpq}(y) \frac{\partial \xi_p^{kl}}{\partial y_q} \right) \frac{\partial \phi_i}{\partial y_j} dy = \int_Y E_{ijkl}(y) \frac{\partial \phi_i}{\partial y_j} dy, \quad \forall \phi \in V_Y, \quad (2)$$

where  $V_Y = \{\phi \in \mathbf{H}_{\text{per}}^1(Y)\}$  is the set of all admissible  $Y$ -periodic displacements.

For the macroscale model of the composite ceramic material we consider a suitable reference domain  $\Omega \subset \mathcal{R}^2$  which can carry given loads. The optimal performance of the biomorphic ceramics strongly depends on the exterior body force  $\mathbf{f}$  and the surface traction  $\mathbf{t}$  applied to a portion  $\Gamma_T \subset \partial\Omega$  of the work-piece. We denote by  $\mathbf{u} = (u_1, u_2)^T$  the displacement vector (state variable), by  $\alpha = (\alpha_1, \dots, \alpha_m)^T$  the design parameters (the widths of the different material layers), and by  $J$  the objective functional to be minimized (e.g., mean compliance, bending strength, etc.). Three different materials ( $m = 3$ ) are considered in the microstructure shown on Fig. 1.

Our optimization problem has the form

$$J(\mathbf{u}, \alpha) = \inf_{\mathbf{v}, \beta} J(\mathbf{v}, \beta), \quad (3)$$

subject to the following equality and inequality constraints on the state variables and the design parameters:

$$\sum_{i,j,k,l=1}^2 \int_{\Omega} E_{ijkl}^H(\alpha) \frac{\partial u_k}{\partial x_l} \frac{\partial \phi_i}{\partial x_j} dx = \int_{\Omega} \mathbf{q} \cdot \phi dx + \int_{\Gamma_T} \mathbf{t} \cdot \phi ds, \quad (4)$$

$$g(\alpha) := \sum_{i=1}^m \alpha_i = C, \quad \alpha_{\min} \leq \alpha_i \leq \alpha_{\max}, \quad 1 \leq i \leq m, \quad (5)$$

where  $\alpha_{\min} = 0$ ,  $\alpha_{\max} = 0.5$ , and  $C$ ,  $0 \leq C \leq 0.5$ , is a given constant. Note that  $\alpha_i = 0$ ,  $1 \leq i \leq m$ , corresponds to a complete void,  $C = 0.5$  to a complete solid material, and the case  $0 < \alpha_i, C < 0.5$ ,  $1 \leq i \leq m$ , corresponds to a microstructural porous composite with a void. Equation (4) refers to the homogenized equilibrium equation given in a weak form.

The constrained minimization problem (3)-(5) is solved by the primal-dual Newton interior-point method. The interior-point aspect is taken care of by

coupling the inequality constraints in (5) by parametrized logarithmic barrier functions whereas the primal-dual aspect stems from coupling the equality constraints by appropriate Lagrangian multipliers. The resulting saddle-point problem is solved by the Newton method applied to the associated Karush-Kuhn-Tucker conditions featuring a line-search approach for the increments and a hierarchy of merit functions for convergence monitoring (see [7]).

### 3 Adaptive Grid Refinement

The main idea of the adaptive grid-refinement process is to find a mesh which is adjusted to the behavior of the solution, i.e., the mesh points have to be concentrated only in those parts of the domain where the solution changes rapidly. For the parts where the solution has unessential changes the mesh is distributed coarsely. This process is usually done by a trial and error analysis. Note that a priori error estimates give information about the asymptotic error behavior and in the case of singularities do not always lead to satisfactory results. In the past twenty years, numerous studies have been devoted to an error control and efficient mesh-design based on some post-processing procedures (cf., e.g., [1, 3, 9–11]). A natural requirement for the a posteriori error estimate is to be less expensive than the computation of the numerical solution. The a posteriori adaptive strategy can be described as follows:

1. Start with an initial coarse mesh  $\mathcal{T}_0$  fitting the domain geometry. Set  $n := 0$ .
2. Compute the discrete solution on  $\mathcal{T}_n$ .
3. Use a posteriori error indicator for each element  $T \in \mathcal{T}_n$ .
4. If the global error is small enough, then **stop**. Otherwise, refine the marked elements, construct the next mesh  $\mathcal{T}_{n+1}$ , set  $n := n + 1$ , and return to step 2.

We solve the linear elasticity equation (2) in the periodicity cell  $Y$  by adaptive finite element method based on the *Zienkiewicz-Zhu* (often called *ZZ*) error estimator proposed in [11]. A detailed theoretical study of the *ZZ*-estimator for linear triangular elements and the Poisson equation can be found in [9]. The basic idea of the method consists in computing an improvement of the solution stress tensor by a post-processing and take the difference between this so-called *recovered continuous stress* and the discrete solution stress as an error estimator. The quality and the reliability of the a posteriori error estimator strongly depend on the approximation properties of the stress recovery technique and the accuracy of the recovered solution.

Assume an initial coarse triangulation satisfying the conditions: i) any two triangles share either a common edge or a common vertex; ii) the triangulation is *shape regular*, i.e., the ratio of the radius of the smallest circumscribed ball to that of the largest contained ball is bounded above by a constant independent of the partition. The adaptive mesh-generation technique essentially depends on the properties of the coarsest mesh. For more details about dealing with hanging nodes within the adaptive procedure and keeping conformity of the elements, we refer, for instance, to [10].

Suppose that for a given level of refinement  $n$  the triangulation  $\mathcal{T}_n$  satisfies the conditions i)-ii). For fixed  $k, l = 1, 2$ , denote by  $\sigma, \hat{\sigma}$ , and  $\sigma^*$ , respectively, the exact stress, the discrete finite element discontinuous stress, and the continuous recovered stress in equation (2) discretized on  $\mathcal{T}_n$ . Originally, the recovered stress was defined in [11] by interpolating the discontinuous (over the elements) approximation  $\hat{\sigma}$  under the assumption to use the same shape functions as for the displacements. This smoothing procedure can be done by nodal averaging method or the  $L_2$ -projection technique. The components of  $\sigma^*$  are piecewise linear and continuous. The computation of the global  $L_2(Y)$ -projection is expensive and hence, as proposed in [11], one usually uses “lumping” of the mass matrix of the form

$$\sigma^*(P) = \sum_{T \in Y_P} \frac{|T|}{|Y_P|} \hat{\sigma}|_T, \quad (6)$$

where  $Y_P \subset Y$  is the union of all elements sharing vertex  $P$ . Thus,  $\sigma^*(P)$  is simply a weighted average of  $\hat{\sigma}$  on the triangles belonging to  $Y_P$ . In practice, local recovery estimators of the form  $\eta_T := \|\sigma^* - \hat{\sigma}\|_{0,T}$  are considered. The global estimator  $\eta_Y := (\sum_{T \in \mathcal{T}_n} \eta_T^2)^{1/2}$  is equivalent to the error  $\|\sigma - \hat{\sigma}\|_{0,Y}$  (we refer to [9, 11] for more details). Heuristically (as an error indicator), the continuous recovered solution  $\sigma^*$  is a better approximation to the exact stress  $\sigma$  than  $\hat{\sigma}$ . In our numerical experiments, we apply (6) only to the boundary grid points  $P \in \partial Y$ . For an arbitrary interior node,  $\sigma^*$  is computed by averaging the stresses at the elements that share the considered node. This procedure requires to solve a least-square problem to find an approximation of the stress at the corresponding vertex inside the domain  $Y$ .

## 4 Numerical Experiments

In this section, we present some results on the computation of the homogenized elasticity coefficients (1) which invokes the numerical solution of (2) with the microcell as the computational domain. Due to the equal solutions  $\xi^{12} = \xi^{21}$ , one has to solve three problems in the period  $Y$  to find  $\xi^{11}$  (Problem 1),  $\xi^{22}$  (Problem 2), and  $\xi^{12}$  (Problem 3). Note that the problem (2) is subjected to periodic boundary conditions on the outer part of  $\partial Y$  and Neumann boundary conditions on the inner part of  $\partial Y$  where the void is located (see Fig.1). For simplicity, we consider a square hole inside the domain and notice that in this case  $E_{2222}^H = E_{1111}^H$ .

We use conforming P1 finite element approximations with respect to an appropriate initial triangulation of  $Y$  and adaptive mesh-refinement procedure based on the ZZ-error indicator. The main purpose of any adaptive algorithm is to get an optimal mesh (heuristically), i.e., to make the discretization errors equidistributed between elements. The following adaptive strategy has been used in our finite element code: mark for refinement those triangles  $T$  for which  $\eta_T \geq \gamma \max_{T' \in \mathcal{T}_n} \eta_{T'}$ ,  $0 < \gamma < 1$  (see Section 3). In our numerical experiments, we choose  $\gamma = 0.5$  as a threshold. The marked elements are refined by a bisection through the marked edge. The problem (2) is solved by the preconditioned

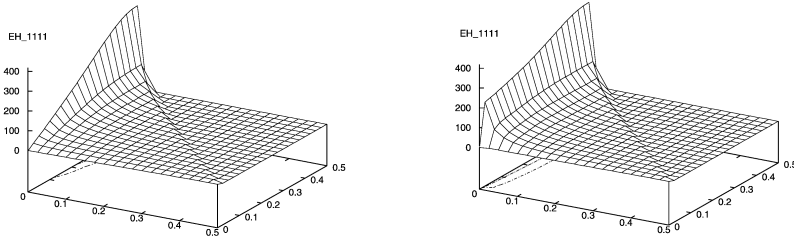


**Fig. 2.** Homogenized coefficients  $E_{1111}^H$  w.r.t. the widths of carbon and SiC layers: a) hole with a weak material; b) hole with no material

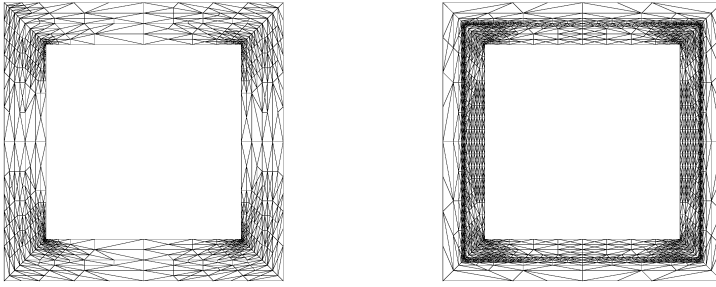


**Fig. 3.** Problem 1, early wood, density = 51%, 9 adaptive refinement levels: a) carbon, 1382 triangles, 737 nodes; b) carbon and SiC, 3754 triangles, 1919 nodes

conjugate gradient (PCG) method with incomplete Cholesky factorization as a preconditioner. Plane stresses are assumed to compute the homogenized elasticity coefficients (1). The Young modulus  $E$  (in GPa) and the Poisson ratio  $\nu$  of our three materials are, respectively,  $E = 10$ ,  $\nu = 0.22$  for carbon,  $E = 410$ ,  $\nu = 0.14$  for SiC, and  $E = 70$ ,  $\nu = 0.17$  for SiO<sub>2</sub>. The numerical examples considered in this section do not take into account the additional thin layer of SiO<sub>2</sub> formed by posttreatment of the SiC-ceramics (after oxidation at high-temperature).

On Fig. 2 we display the behavior of the homogenized coefficient  $E_{1111}^H$  versus the widths of the C and SiC layers which vary between 0 and 0.5. The first picture a) on this figure treats the void as a weak material with  $E = 0.01$  and  $\nu = 0.45$  whereas b) concerns a complete void with no material. We compute the effective coefficients  $E_{ijkl}^H$  only for a fixed number of values of the design parameters (e.g.,  $20 \times 20$  grid as shown on Fig. 2) and then interpolate the values by splines. With regard to the homogenized state equation (4), this procedure results in having explicit formulas at hand for the gradients and the Hessian of the Lagrangian function needed in the optimization loop (see [7]).

The mesh-adaptive process is visualized on Figures 3 and 4. We see that in case a) of one material available in the microstructure, an appropriate refinement is done around the corners where the hole with a complete void is located. In case b) of more materials, additional mesh-adaptivity is needed across the material

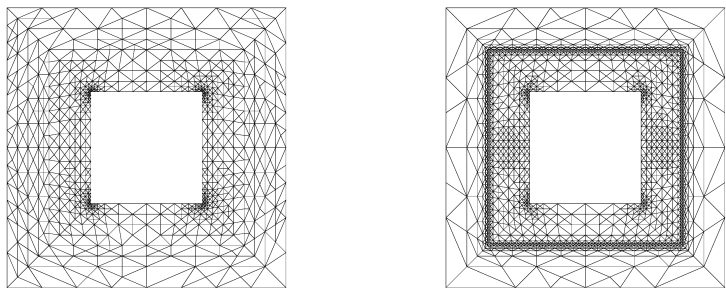


**Fig. 4.** Problem 1, late wood, density = 84%, 9 adaptive refinement levels: a) carbon, 1527 triangles, 818 nodes; b) carbon and SiC, 3752 triangles, 1916 nodes

**Table 1.** Homogenized coefficients (early wood) w.r.t. adaptive refinement level

level	$E_{1111}^H$	$E_{1122}^H$	$E_{1212}^H$	nt / nn (Prob.1,2)	nt / nn (Prob.3)
1	64.975	7.664	12.116	168 / 100	168 / 100
2	63.336	6.642	9.750	220 / 126	224 / 128
3	58.466	6.682	8.073	288 / 162	300 / 168
4	56.572	7.012	6.643	484 / 262	576 / 308
5	54.385	6.245	6.212	712 / 378	760 / 402
6	52.936	6.091	5.474	1208 / 630	1376 / 716
7	51.914	5.458	5.306	1800 / 932	1800 / 930
8	50.861	4.790	5.217	2809 / 1444	2688 / 1374
9	50.455	4.571	5.029	3754 / 1919	3726 / 1896
10	49.591	4.359	4.983	5918 / 3013	5708 / 2896

interfaces in the microstructure due to the strongly varying material properties (Young’s modulus and Poisson’s ratio). The ZZ a posteriori error estimator is local, not expensive and yields satisfactory results as the numerical experiments show. We also note that the density of the microcell depends on the *growing state* of the wood. In early wood regions (growth of the tree in spring and summer) the holes are large and the cell walls are thin (see Fig. 3, density 51%). For the late wood regions (autumn), the density of the tracheidal cells is larger compared to the early tree due to the smaller pores and the ticker cell walls, see Fig. 4.

In Table 1 we give some results for the homogenized elasticity coefficients on various adaptive refinement levels in the case of early wood. We report the number of triangles **nt** and the number of nodes **nn** on each level when solving problems (2). The corresponding experimental data in the case of late wood are presented in Table 2. We see from both Tables that the mesh sensitivity on the successive levels is very small. Our adaptive mesh-refinement procedure stops when a priori given limit for the number of refinement levels is reached.



**Table 2.** Homogenized coefficients (late wood) w.r.t. adaptive refinement level

level	$E_{1111}^H$	$E_{1122}^H$	$E_{1212}^H$	nt / nn (Prob.1,2)	nt / nn (Prob.3)
1	33.430	3.885	9.893	168 / 100	168 / 100
2	33.064	3.929	9.577	216 / 126	224 / 128
3	32.844	4.024	9.283	300 / 168	284 / 160
4	32.291	4.254	8.970	544 / 296	520 / 280
5	32.144	4.312	8.809	828 / 438	668 / 356
6	31.909	4.372	8.703	1354 / 705	1064 / 556
7	31.862	4.379	8.526	1892 / 980	1484 / 768
8	31.735	4.399	8.470	2894 / 1485	2232 / 1142
9	31.711	4.400	8.373	3752 / 1916	3088 / 1576
10	31.487	4.497	8.321	5716 / 2906	4564 / 2316

Acknowledgements

This work has been partially supported by the German NSF (DFG) under Grant No.HO877/5-2. The second author has also been supported in part by the Bulgarian NSF under Grant I1001/2000.

References

1. Babuska, I., Miller, A.: A feedback finite element method with a posteriori error estimation: Part I. The finite element method and some basic properties of the a posteriori error estimator. *Comput. Methods Appl. Mech. Eng.*, **61** (1987) 1–40.

2. Bakhvalov, N., Panasenko, G.: *Averaging Processes in Periodic Media*. Nauka, Moscow, 1984.

3. Becker, R., Kapp, H., Rannacher, R.: Adaptive finite element methods for optimization problems. *Numerical Analysis*, **39** (1999) 21–42.

4. Bendsoe, M. P., Kikuchi, N.: Generating optimal topologies in structural design using a homogenization method. *Comput. Methods Appl. Mech. Eng.*, **71** (1988) 197–224.

5. Bensoussan, A., Lions, J. L., Papanicolaou, G.: *Asymptotic Analysis for Periodic Structures*. North-Holland, Elsevier Science Publishers, Amsterdam (1978)

6. Greil, P., Lifka, T., Kaendl, A.: Biomorphic cellular silicon carbide ceramics from wood: I. Processing and microstructure, and II. Mechanical properties. *J. Europ. Ceramic Soc.*, **18** (1998) 1961–1973 and 1975–1983.

7. Hoppe, R. H.W., Petrova, S. I.: Homogenization Design Method for Biomorphic Composite Materials. *J. Comput. Methods Sci. Eng.*, **3** (2003) 383–391 (to appear).

8. Jikov, V. V., Kozlov, S. M., Oleinik, O. A.: *Homogenization of Differential Operators and Integral Functionals*. Springer (1994)

9. Rodriguez, R.: Some remarks on Zienkiewicz-Zhu estimator. *Numer. Methods Partial Differential Equations*, **10** (1994) 625–635.

10. Verfürth, R.: A posteriori error estimation and adaptive mesh-refinement techniques. *J. Comput. Appl. Math.*, **50** (1994) 67–83.

11. Zienkiewicz, O. C., Zhu, J. Z.: A simple error estimator and adaptive procedure for practical engineering analysis. *Intern. J. Numer. Methods Eng.*, **24** (1987) 337–357.